Received: 11 August 2023 | Revised: 15 September 2023 | Accepted: 22 September 2023

DOI: 10.1002/elan.202300238

RESEARCH ARTICLE

ELECTROANALYSIS

Sensitive and selective determination of the neonicotinoid nitenpyram utilizing capillary electrophoresis hyphenated to amperometric detection/mass spectrometry

M. Koall.[1] | **D. Böhm**[1] | **T. Herl**[2] | **F.-M. Matysik**[1]

[1]University of Regensburg, Faculty of Chemistry and Pharmacy, Institute of Analytical Chemistry, Chemo- and Biosensors, Regensburg, Germany

[2]University of Regensburg, Faculty of Chemistry and Pharmacy, Central Analytical Department, Regensburg, Germany

Correspondence
F.-M. Matysik, University of Regensburg, Faculty of Chemistry and Pharmacy, Institute of Analytical Chemistry, Chemo- and Biosensors, Universitätsstraße 31, 93053 Regensburg, Germany.
Email: Frank-Michael.Matysik@chemie.uni-regensburg.de

Funding information
Deutsche Forschungsgemeinschaft (DFG, German research foundation), Grant/Award Number: MA1491/12-1

Abstract

In this work, we present the sensitive and selective determination of the widely used insecticide nitenpyram (NIT), utilizing a newly developed dual detection concept (DDC) for capillary electrophoresis (CE). This DDC was realized by combining two complementary detection principles, namely amperometric detection (AD) and mass spectrometry (MS), using a commercially available flow splitter (CE-AD/MS). The novel DDC was implemented utilizing a newly developed, modular, and user-friendly CE system with a unique capillary positioning mechanism to improve the workflow. A detailed description of the CE device can be found in the Supporting Information.

We investigated the analytical performance of the novel DDC (CE-AD/MS) in the context of NIT determination.

The NIT LOD, obtained by AD, was up to a factor of 14 lower than in case of MS in the context of CE-AD/MS. The qualitative and quantitative determination of NIT in pharmaceutical samples is presented as a possible application for the novel DDC. Additionally, the oxidation process during AD was examined by hyphenation of electrochemistry to CE-MS.

KEYWORDS
dual detection, electrochemistry, electrophoresis, mass spectrometry, nitenpyram

1 | INTRODUCTION

Neonicotinoids (neonics) are systematic neurotoxins whose mechanism of action is based on the irreversible binding of the neonic to the nicotinic acetylcholine receptors of the central nervous system of insects. Thus, neonics can be applied to combat a wide range of target organisms [1]. High efficiency, good water solubility, and low toxicity to mammals make them formidable tools for pest control in agriculture and veterinary medicine [2, 3].

However, this great advantage can also become a problem, especially if the insecticide not only eliminates the actual pests but also negatively influences non-target organisms. Recent studies highlighted the adverse effects of neonics on different bee species, which are important pollinators for many ecosystems [4]. Further studies indicate that there is an increased risk potential for humans due to the increasing use of some neonics. Several neonics and their degradation products have shown the ability to interact with human cells and cause dysfunctionalities in the human nervous system and the human genome [5].

Nitenpyram (NIT) is a widely used representative of the neonic substance class. It is used in agriculture for seed coating and spraying against many types of aphids and plant hoppers [3, 6]. In veterinary medicine, it can be used effectively against fleas and ticks when applied orally [2]. When NIT is applied to soil, plants, or animals, it can be released into the environment and cause lasting damage to non-target insects, earthworms [7], and, consequently, whole ecosystems which rely on them. Therefore, complying with the legal limit values when NIT is used is important. In this context, monitoring the NIT content in chemical and pharmaceutical products or agriculture is mandatory.

For this purpose, sensitive and reliable analytical methods are of central importance. Nowadays, the determination of NIT is commonly achieved by liquid chromatography (LC) hyphenated to either UV/VIS detection [8, 9], fluorescence detection [10], or mass spectrometry [11, 12] (MS). As an alternative approach, capillary electrophoresis (CE) hyphenated to MS using an alkaline aqueous background electrolyte was reported by Sánchez-Hernández et al. [12]. Here, NIT migrated near the electroosmotic flow, which could complicate a selective determination.

A novel dual detection concept (DDC), developed by Böhm et al. [13], could also be promising in NIT monitoring. In this concept, non-aqueous CE is coupled with amperometric detection (AD) and MS (CE-AD/MS). The parallel arrangement of AD and MS, which are both destructive detection methods, was achieved by a commercially available flow splitter. This concept combines the high separation efficiency and low sample consumption of CE with two detectors providing complementary information about the sample [13, 14]. AD is among the most sensitive detection methods for electroactive analytes and shows good reproducibility and long-term stability in non-aqueous media [15]. Therefore, it is ideally suited for the quantification of low concentrations [14]. However, only limited qualitative information is obtained by AD [16]. MS is a powerful technique when it comes to the identification of unknown or co-migrating analytes [13]. Furthermore, the risk of false positives in the resulting electropherograms is eliminated by the DDC as the composition of each peak can be monitored by MS. The possibility of interferences is also minimized since CE is a powerful separation technique for charged analytes, providing a very selective migration behavior for NIT in nonaqueous background electrolyte. Consequently, the combination of these two detection principles hyphenated to CE can lead to a powerful DDC for the simultaneous identification and quantification of many analytes.

In this study, the novel DDC CE-AD/MS was characterized in the context of NIT determination. To optimize the method workflow, a novel modular CE system was developed. It was possible to detect NIT selectively in a mixture of six commonly used neonics. With the excellent sensitivity of AD, very low detection limits could be achieved by the DDC. Furthermore, the oxidation process during AD was examined by means of electrochemistry hyphenated to CE-MS (EC-CE-MS). The DDC was successfully utilized for the quantification of NIT in pesticide pills.

2 | EXPERIMENTAL

2.1 | Reagents and materials

The following chemicals were used, all of analytical grade: Acetamiprid (ACA), clothianidin (CLO), imidacloprid (IMI), nitenpyram (NIT), thiachloprid (TCL), and thiamethoxam (TMX) were purchased from Sigma-Aldrich (St. Louis, USA). Acetonitrile (ACN), ammonium acetate, 0.1 M sodium hydroxide solution, and formic acid were purchased from Merck (Darmstadt, Germany). Ferrocenemethanol (FcMeOH) was purchased from ABCR (Karlsruhe, Germany). Acetic acid was purchased from Carl Roth (Karlsruhe, Germany). Capstar™ 11,4 mg pills for pets were supplied by Elanco (Bad Homburg, Germany). Ultrapure water was provided by a Milli-Q Advantage A10 system (Merck Darmstadt, Germany).

All measurements were carried out using a background electrolyte consisting of 1 M acetic acid and 10 mM ammonium acetate in ACN (ACN BGE).

Fused silica capillaries (50 μm inner diameter, 365 μm outer diameter, polyimide coated) were purchased from Polymicro Technologies (Phoenix, USA). The FS CapTite Interconnect Y C360-203Y–U-C100 and the corresponding fitting CapTite One-Piece Fitting C360-100 were obtained from LabSmith (Livermore, USA).

2.2 | Instrumentation

2.2.1 | CE system and novel capillary positioning concept

For the implementation of the DDC (CE-AD/MS), a newly developed modular CE system was used. It was equipped with a novel capillary positioning mechanism, allowing the utilization of silicone septa and pressure-assisted injection. A detailed view of the setup (Figure S1) and a detailed description of the laboratory-constructed CE system can be found in the Supporting Information.

The most important feature of the CE system was the unique capillary positioning mechanism which was used

in combination with a rotating sample tray. In Figure 1, the capillary positioning system is shown in detail.

The electrode arm (Figure 1, a) and the capillary arm (Figure 1, b) were connected to threaded rods (Figure 1, c) driven by stepper motors placed in the lower part of the CE device. The arms could be controlled by the software and moved independently. The capillary (Figure 1, d) was installed by a micro-tight fitting (Figure 1, e). A funnel-shaped and gas-tight holder for the cannula (Figure 1, f) was attached to the cannula arm. The cannula (0.80/40 mm diameter/length, Figure 1, g) from B. Braun (Melsungen, Germany) was connected to the holder via a bayonet lock which was milled into the lower part of the holder, allowing a fast replacement. The cannula could be used to pierce a silicone septum and served as a guiding system for the capillary. Additionally, the stainless steel part was connected to the high-voltage source T1CP 300 304p from ISEG (Radeberg, Germany) via an insulated cable (Figure 1, h) and served as a high-voltage electrode. On top, the holder was equipped with a screw cap ND 13 LC41.1 with integrated silicone septum E158.1 from Carl Roth (Karlsruhe, Germany, Figure 1, i). The capillary was guided through the middle of the septum, into the funnel-shaped holder and through the attached capillary guiding. With this positioning system, the relative positioning of the capillary and high-voltage electrode could be optimized for the corresponding task. For the injection from a standard sample vial, the cannula pierced the septum but stopped inside the gas phase so that only the capillary was immersed in the sample solution to minimize the risk of sample carryover. During CE separation, the electrode dipped into the background electrolyte. The capillary protruded about 2 mm from the tip of the cannula. Furthermore, with individual positioning, it was possible to use various vial types and micro-inserts simultaneously. This setup allowed the flushing of the capillaries or pressure-assisted injection of the sample.

An improved electrochemical injection cell, based on disposable electrodes, was developed for EC-CE-MS measurements. It is schematically shown in Figure 2.

The cell was equipped with a thin-film electrode system with platinum working, counter, and pseudo-reference electrodes (ED-SE1-PT, Micrux Technologies, Oviedo, Spain, Figure 2, a). The electrode was connected to a μAutolab potentiostat/galvanostat (Metrohm Autolab B. V., Utrecht, Netherlands) via spring-loaded pins. All potentials given are referred to the Pt pseudo-reference electrode and all electrochemical measurements were carried out in ACN

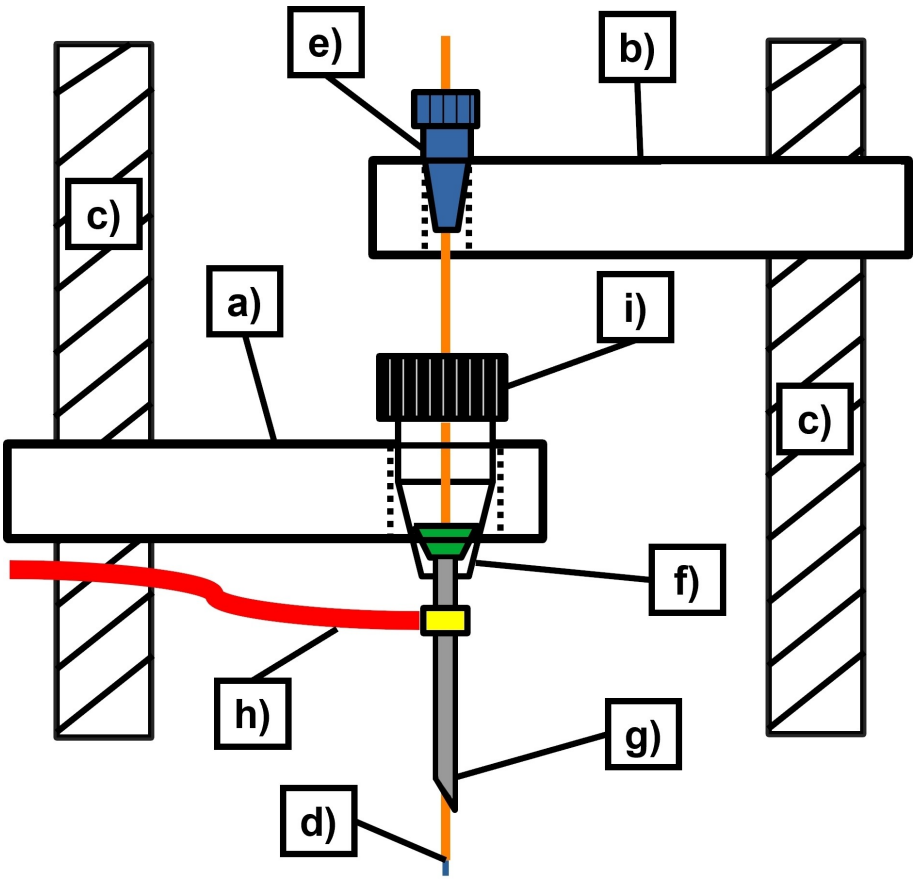

FIGURE 1 Sketch of the electrode and capillary positioning mechanism. a) cannula arm, b) capillary arm, c) threaded rods, d) capillary, e) micro-tight fitting, f) cannula holder, g) cannula, h) high voltage cable, and i) screw cap with integrated silicone septum.

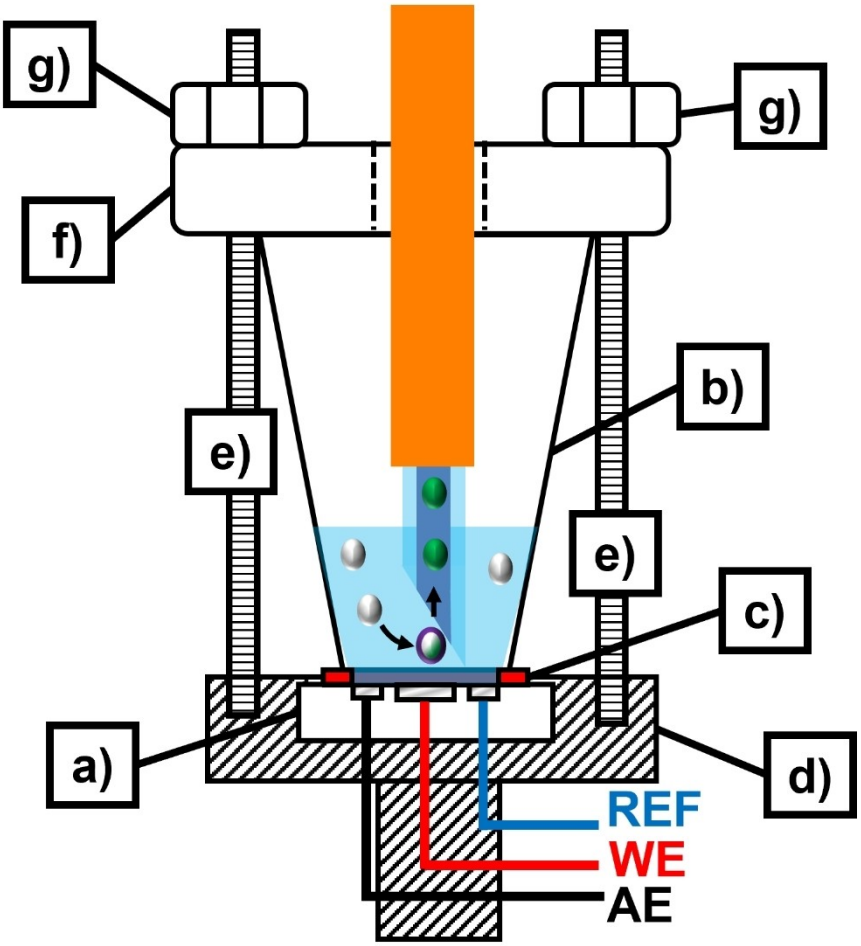

FIGURE 2 Sketch of the laboratory-constructed injection module for EC-CE-MS. Components: a) Micrux chip electrode, b) cut micro-insert, c) silicone gasket, d) aluminum baseplate, e) threaded rods, f) PTFE top plate, and g) hex nuts.

BGE. The sample volume was filled into a modified 100 µL micro insert (VWR International b. v., Leuven, Belgium, Figure 2, b). A silicone septum E158.1 from Carl Roth (Karlsruhe, Germany) with an inner hole (Figure 2, c) served as a gasket between the electrode and micro-insert. The electrode and insert were sealed with the gasket using a laboratory-constructed clamping device (Figure 2, d–g). The injection cell could be placed in the autosampler of the CE, analogous to a standard vial. For the injection of the sample from the electrode surface, the position of the high-voltage electrode and capillary were optimized with the help of the capillary positioning system.

2.2.2 | CE-AD/MS setup

In this project, we used CE hyphenated to parallel AD and MS detection (CE-AD/MS). The DDC [13] and the laboratory-constructed AD cell [17] are described elsewhere in detail.

Briefly, a parallel arrangement of the two destructive detectors could be achieved by utilizing a commercially available y-shaped flow splitter (FS) with a dead volume of 9 nL and a through-hole diameter of 100 µm. This method allowed a dead-volume-free flow splitting and synchronization of the migration times for both detectors [13, 14]. A detailed description of different FSs can be found in our previous work [13].

For AD, a user-friendly cell design of a three-electrode system was used. Two symmetrically arranged stainless steel tubes served as a guiding system for the separation capillary and a 25 µm Pt disk electrode. An Ag/AgCl electrode served as a reference electrode. The stainless-steel tube, which was used as capillary guiding, served as an auxiliary electrode for the AD cell and was grounded to close the CE circuit. The electrodes were positioned using an UltraZoom Pro digital microscope from dnt (Dietzenbach, Germany). The electrodes were connected to an SP-200 potentiostat equipped with an ultralow current module from BioLogic (Seyssinet-Pariset, France). The AD

cell was kept in a laboratory-constructed Faraday cage to prevent electromagnetic interference.

A micrOTOF from Bruker Daltonics (Bremen, Germany) with a coaxial sheath liquid ESI interface from Agilent Technologies (Santa Clara, USA) was used for MS detection. The device was operated with the following parameters: positive ion polarity mode, nebulizer gas pressure 2 bar, dry gas (N_2) flow 4 L/min, dry gas temperature 250 °C, and *m/z* 50–600. The sheath liquid had a flow rate of 8 µl/min and consisted of water, 2-propanol, and formic acid (49.9 : 49.9:0.2, v/v/v).

All components of the DDC were connected by three fused silica capillaries (inner diameter 50 µm, lengths: in front of the FS 30 cm, after FS 35 cm). To allow simultaneous detection of the neonics at both detectors, the AD cell was positioned 5 cm lower than the ESI interface.

Prior to the CE-AD/MS setup assembly, 5 mm of the polyimide coating of the capillary tips was removed, and the tips were polished to a 90° angle. Subsequently, the capillaries were conditioned by flushing them for 10 min with 0.1 mM sodium hydroxide solution, followed by 5 min with ultrapure water and 30 min with ACN BGE.

2.2.3 | EC-CE-MS setup

EC-CE-MS was used for the investigation of the oxidation process during AD. The CE system was equipped with the newly developed electrochemical injection cell and hyphenated to a Q-TOF-MS system (model 6540, Agilent Technologies, Santa Clara, USA) equipped with a coaxial sheath liquid ESI interface from Agilent Technologies (Santa Clara, USA). The device was operated with the following parameters: positive ion polarity mode, dry gas temperature 250 °C; dry gas flow 8 L min^{-1}; nebulizer gas pressure 2.8 bar; sheath gas flow 6 L min^{-1}. The sheath liquid had a flow rate of 8 µl/min and consisted of water, 2-propanol, and formic acid (49.9 : 49.9:0.2, v/v/v). The Q-TOF was chosen for the identification of the unknown species because it provided a higher mass accuracy and a superior mass resolution compared to the micrOTOF.

The sample was hydrodynamically injected for 10 s from the electrode surface into a fused silica capillary (length: 50 cm, inner diameter: 50 µm, preconditioning as in section 2.2.2). The capillary tip was polished to a 30° angle to allow flow into the capillary when the tip was in contact with the working electrode.

2.2.4 | Software

The measurement data were evaluated with Origin 2022 from OriginLab (Northampton, USA), Data Analysis 4.0 SP1 from Bruker Daltonics (Bremen, Germany), MassHunter™ workstation software for 6500 series Q-TOF version B9.0.9044.0, MassHunter™ workstation Qualitative Analysis version 10.0 from Agilent Technologies (Santa Clara, USA) and EC-Lab V11.43 from BioLogic (Seyssinet-Pariset, France). The CE system was operated by Labview-based software.

2.3 | Experimental procedures

2.3.1 | Sample preparation

A sample solution consisting of 0.1 mM ACA, CLO, IMI, NIT, TCL, and TMX in ACN BGE was prepared as a model system for the novel DDC.

For the determination of the LOD of CE-AD/MS for NIT, sample solutions with concentrations ranging from 100 nM to 500 mM were prepared.

For the investigation of the insecticide pill, calibration solutions of NIT in ACN BGE (10 to 60 mg/L) were prepared. The pill was extracted using a UP50/100 ultrasonic processor from Hielscher Ultrasonics (Teltow, Germany), equipped with an MS3 sonotrode, using 30 ml pure ACN as solvent. The pill extract was filtered by a syringe filter (ROTILABO® 0.45 µm, PTFE, Carl Roth, Karlsruhe, Germany) to remove non-dissolved particles. Afterward, the ACN was removed from the filtrate by evaporation, and the residue was dissolved in BGE used in CE (1 M acetic acid, 10 mM ammonium acetate in ACN). This protocol was applied to minimize the carryover of possible interfering substances that were used in the formulation, as acetic acid and ammonium acetate could enhance the solubility of many compounds in ACN. After dilution to a target concentration of about 0.1 mM, the NIT content was determined utilizing CE-AD/MS.

Sample solutions with an NIT content of 0.1 mM in ACN BGE were prepared to investigate the NIT oxidation.

2.3.2 | CE-AD/MS measurements

The AD cell was filled with ACN BGE before the measurements. Subsequently, the potential shift in the AD cell caused by the CE circuit was determined and compensated according to the method described by Böhm et al. [13]. The sample was injected hydrodynamically for 20 s. The separation voltage was 25 kV. Prior to each CE-AD/MS measurement, an electrode pre-treatment protocol (2.5 V for 10 s followed by −0.5 V for 10 s) was used to avoid electrode fouling of the AD working electrode. Subsequently, the detection potential of 1.7 V (corrected potential in the presence of high-voltage) was applied.

2.3.3 | EC-CE-MS measurements

The injection cell was filled with 75 µl of 0.1 mM NIT in ACN BGE before the measurements. The injection was performed hydrodynamically for 10 s, whereby a potential was applied to the working electrode of the injection cell. Oxidation potentials from 1.6 V to 2.0 V were investigated.

3 | RESULTS AND DISCUSSION

3.1 | Determination of various neonics utilizing the novel DDC (CE-AD/MS)

The new DDC was tested for a selection of the most widely used neonics for pest control, namely ACA, CLO, IMI, NIT, TCL, and TMX. Preliminary ESI-TOF-MS measurements were performed, whereby the sample was injected directly via a fused silica capillary to determine the *m/z* values, which were used to identify the respective neonic in subsequent measurements. For all six neonics, the protonated molecule $[M+H]^+$ was the predominant signal in the obtained mass spectrum. In Table 1, the results of the mass spectrometric characterization are summarized.

Subsequently, a mixture containing 0.5 mM ACA, CLO, IMI, NIT, TCL, and TMX was investigated utilizing CE-AD/MS (see Figure 3).

The electropherogram at the top (red), which was recorded with AD, shows one peak in the migration window for cationic species. The second s-shaped signal can be assigned to the electroosmotic flow (EOF). The set of electropherograms at the bottom (blue) was recorded with ESI-TOF-MS and shows the extracted ion electropherograms with *m/z* values from Table 1. Based on that, the cationic signal can be assigned to NIT using MS (*m/z* 271.1). Furthermore, differences in the peak heights of the different species are observable. A possible reason for this observation could be the different ionization efficiencies of the neonics. NIT shows the highest ionization efficiency, corresponding to the largest peak height of all investigated neonics, while CLO, TCL, and TMX show smaller signals related to a lower ionization efficiency. Comparing both electropherograms, some conclusions can be made. Firstly, only the migration time for NIT enables a good separation, meaning NIT is positively charged, hence partially protonated in ACN BGE. The higher degree of protonation could also contribute to the higher ionization efficiency of NIT. Secondly, only NIT shows a distinct amperometric response, leading to the conclusion that NIT can be selectively detected with AD and MS simultaneously. In summary, while it is not applicable to the other investigated neonics as they can neither be separated by CE nor detected by AD, the method is ideally suited for the analysis of NIT.

TABLE 1 Names, abbreviations, formulas, and base peaks of the respective protonated species $[M+H]^+$ obtained by direct injection to ESI-TOF-MS.

Neonic	Abbreviation	Formula	$[M+H]^+$ [Da]
Acetimprid	ACA	$C_{10}H_{11}ClN_4$	223.3
Clothianidin	CLO	$C_6H_8ClN_5O_2S$	250.2
Imidacloprid	IMI	$C_9H_{10}ClN_5O_2$	256.3
Nitenpyram	**NIT**	$\mathbf{C_{11}H_{15}ClN_4O_2}$	**271.1**
Thiacloprid	TCL	$C_{10}H_9ClN_4S$	255.3
Thiamethoxam	TMX	$C_8H_{10}ClN_5O_3S$	292.0

3.2 | Analytical performance of the DDC (CE-AD/MS) in NIT determination

With the first proof-of-concept for selective NIT determination, the following aspect addressed in this study was the detectability of NIT within the new DDC. The LODs of NIT detection were investigated for the DDC, as well as for single AD, to determine whether the flow splitting introduced a loss of sensitivity. The LODs of CE-AD/MS and single AD were determined for an S/N of 3 and are listed in Table 2.

The NIT LOD of 500 nM, obtained by AD, was up to a factor of 14 lower than for MS in the context of the DDC (CE-AD/MS). Table 3 shows a comparison with other instrumental methods which are commonly used for NIT determination.

Methods such as CE or LC coupled with MS/MS or LC coupled with fluorescence detection show lower LODs compared to CE-AD/MS (see Table 3). However, these are more complex to implement instrumentally, for example in the case of MS/MS detection [11, 12], or involve additional critical steps, such as the derivatization of the analytes in fluorescence detection [10]. CE-AD/MS is easy to implement, requires no additional derivatization steps, and shows a significantly lower LOD than LC hyphenated to UV detection, which is similar in terms of user-friendliness.

TABLE 2 LODs for the DDC (CE-AD/MS) and single detection (CE-AD) for NIT in ACN BGE ± SD (n = 3).

LOD	AD	MS
LODs DDC [µM]	0.50 ± 0.08	7.3 ± 1.4
LODs single detection [µM]	0.48 ± 0.05	–

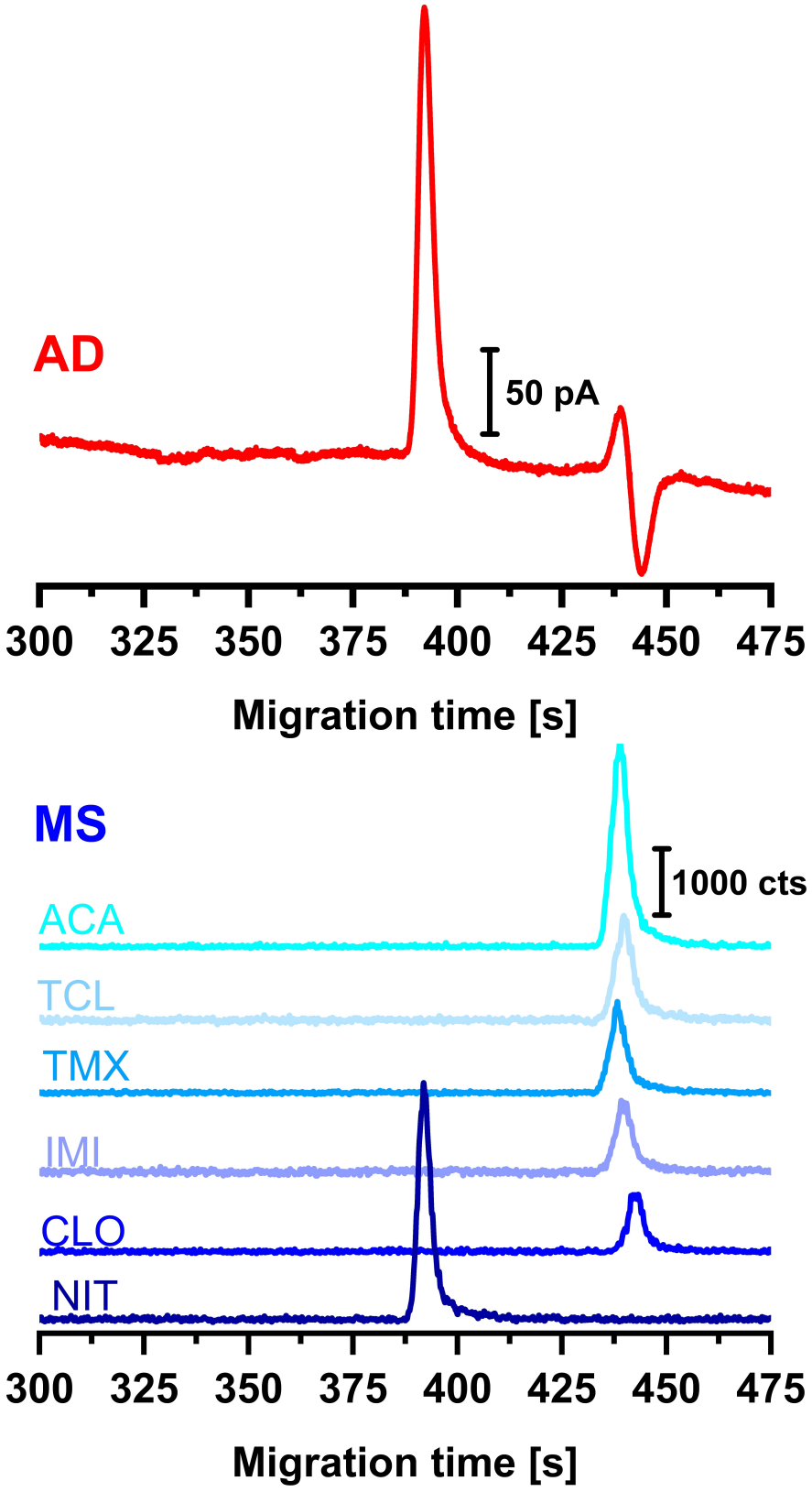

FIGURE 3 CE-AD/MS measurement of a mixture of 0.5 mM ACA, CLO, IMI, NIT, TCL, and TMX in ACN BGE. The electropherogram at the top was recorded with AD at 1.7 V, and the extracted ion electropherograms at the bottom were recorded with MS. For MS detection, the *m/z* values for the corresponding neonics were taken from Table 1.

An exemplary measurement of 50 μM NIT is shown in Figure 4 to demonstrate the different S/N ratios of MS and AD detection.

FcMeOH was added as an EOF marker. Despite the difference in sensitivity, it was possible to identify both substances using MS. This is important to check peak purity as co-migrating analytes can lead to false results in AD. The performance of the two detectors was excellent for their respective task in the DDC (CE-AD/MS) (MS was used for identification and AD for quantification). Comparing the LODs of AD in the DDC and single AD in Table 2, there is no significant loss of sensitivity induced by flow splitting. Based on these results, the novel DDC (CE-AD/MS) could be used to ensure a selective and sensitive NIT determination.

TABLE 3 LODs of the most common instrumental methods for NIT determination.

Detection method	Separation method	LOD [μg/L]	Source
Fluorescence detection	LC	0.1	[9]
UV/VIS detection	LC	50000	[10]
MS (MS/MS) detection	CE [12], LC [11]	2.2 [12] 0.1 [11]	[11, 12]
CE-AD/MS	**CE**	**135**	**This work**

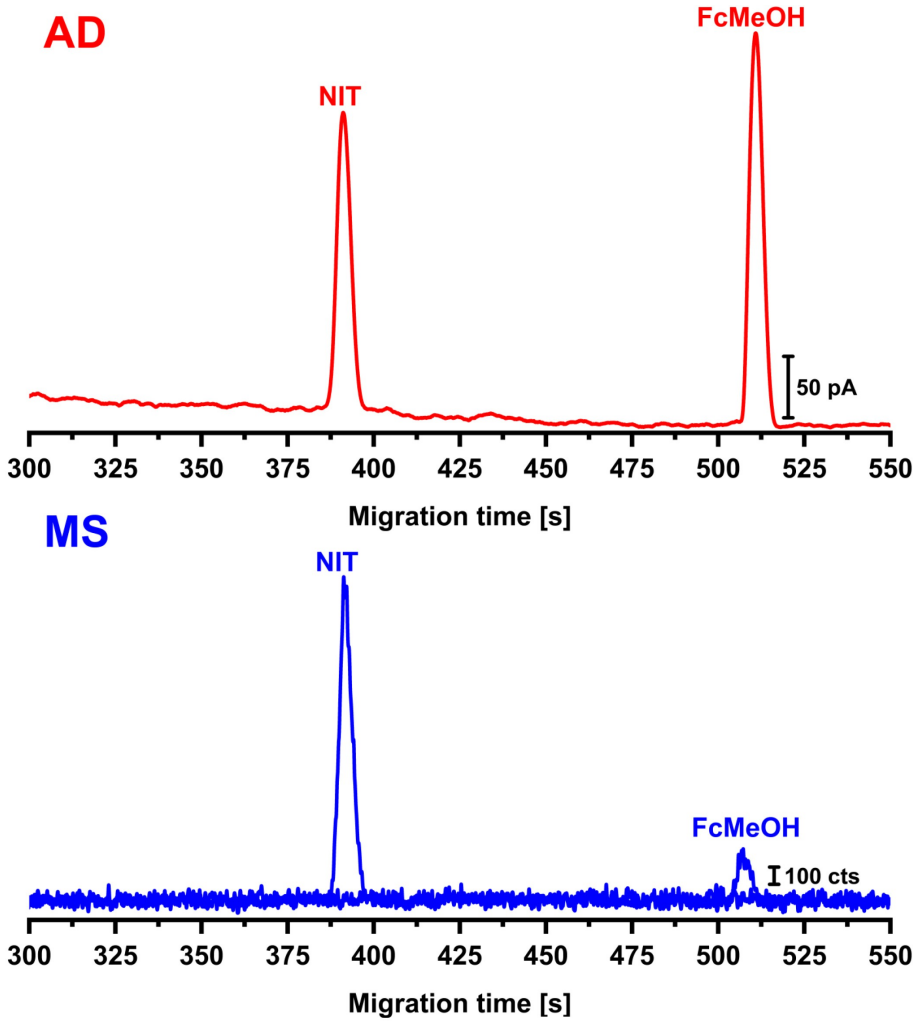

FIGURE 4 CE-AD/MS measurement of a mixture of 0.05 mM NIT and FcMeOH in ACN BGE. The electropherogram at the top was recorded with AD, and extracted ion electropherograms for *m/z* 199.0 (FcMeOH) and *m/z* 271.1 (NIT) recorded with MS.

3.3 | Detection of NIT in pesticide pills for pets

Quality control is an essential task in the chemical and pharmaceutical industry. It is mandatory to ensure the purity and proper dosage of active substances in complex products to guarantee a safe application. NIT is a compound used in veterinary medicine. Therefore, certain concentration and purity standards must be fulfilled. With its high sensitivity and the option to identify possible impurities, the DDC may have great potential in this field. As an example, we examined commercially available pesticide pills for pets. The electropherograms of a pill sample are depicted in Figure 5.

The electropherograms for AD (Figure 5, top, red) and MS (Figure 5, bottom, blue) showed only one signal. The signal was identified as NIT (*m/z* 271.1, see Table 1) using MS. The NIT content of the extract was quantified using the AD signal and external calibration. The corresponding calibration curve is shown in the Supporting Information (Figure S2). Quantitation of the AD signal resulted in a mass concentration of 28.6 ± 0.6 μg/ml. Thus, after applying our extraction protocol and subsequent CE-AD/MS measurements, we detected 11.4 ± 0.3 mg per pill. This agrees very well with the manufacturer's information on an NIT content of 11.4 mg, reaching a recovery rate of 100 %.

3.4 | EC-CE-MS studies of NIT

EC-CE-MS measurements at different potentials were performed to better understand the oxidation processes during the amperometric detection. In the EC-CE-MS experiments, Pt was used as a pseudo-reference electrode. The extracted ion electropherograms shown in Figure 6 were obtained with oxidation potentials ranging from 1.6 V to 2.0 V vs. Pt.

The extracted ion electropherograms represent different species which were characterized by their respective *m/z* values. From the electropherograms, the following observation could be made. At 1.6 V, no signal other than NIT (*m/z* 271.092, see Table 1) was detected. Starting at 1.7 V, three electrochemically generated species at *m/z* 270.096 (Figure 6, red), *m/z* 258.096 (Figure 6, blue), and *m/z* 141.111 (Figure 6, orange) were detected. Further experiments indicated that *m/z* 141.111 was related to the ACN BGE, as the signal was also present when bare ACN BGE was oxidized at 2 V (see Figure S4). All species showed a faster migration in the migration window for cationic species compared to NIT, leading to the conclusion that all electrochemically generated products were cationic or protonated species. For a further investigation of the electrochemically generated species, the mass spectra of the peaks were extracted (see Figure S5 A–D). Based on the mass spectra of the oxidation products, the molecular formulas of the respective compounds were obtained utilizing the embedded tool of the MassHunter™ software. The significant parameters and resulting empirical formulas are shown in Table 4.

$C_{12}H_{17}ClN_3O_2$ (*m/z* 270.096) and $C_{11}H_{16}ClN_3O_2$ (*m/z* 258.096) could be assigned to the oxidation of NIT. The computed empirical formula $C_6H_9N_3$ (*m/z* 141.111) could be assigned to an NH_4^+ adduct of an ACN-based polymer. Similar polymers have been reported by Oprea et al. [18] for mechanically initiated polymerization of ACN. The simulated spectra of the proposed sum formulas are also displayed in Figure S5 A–D for a comparison with the experimental data. The experimental data agree well with the simulated spectra for all investigated products.

4 | CONCLUSIONS

In this manuscript, we described a reliable, selective, and sensitive NIT determination utilizing the novel DDC CE-AD/MS. We were able to detect NIT selectively in a mixture of six neonics commonly used in agriculture and veterinary medicine. In these studies, a selective migration time and a pronounced electrochemical activity in ACN BGE could be observed for NIT. We showed the possibility of detecting NIT simultaneously with AD and MS after CE

TABLE 4 Base peaks of the mass spectra, migration times ± SD, empirical formulas, relative TOF-MS *m/z* errors, and isotope pattern match for NIT (*m/z* 271.092) and oxidation products (*m/z* 270.096, *m/z* 258.096 and *m/z* 141.111) obtained by EC-CE-MS measurements shown in Figure 6. Empirical formulas, relative TOF-MS *m/z* errors, and ionization pattern match data were reported as determined by the MassHunter™ software.

Base peak m/z [Da]	Migration time [s]	Empirical formula	Ionization	Relative TOF-MS *m/z* error [ppm]	Isotope pattern match [%]
271.0.92	207 ± 3.9	$C_{11}H_{15}ClN_4O_2$	$[M+H]^+$	0.99	97.9
270.096	160 ± 2.3	$C_{12}H_{17}ClN_3O_2$	$[M]^+$	0.07	99.9
258.096	168 ± 2.5	$C_{11}H_{16}ClN_3O_2$	$[M+H]^+$	0.34	86.7
141.111	191 ± 2.5	$C_6H_9N_3$	$[M+NH_4]^+$	−3.83	77.5

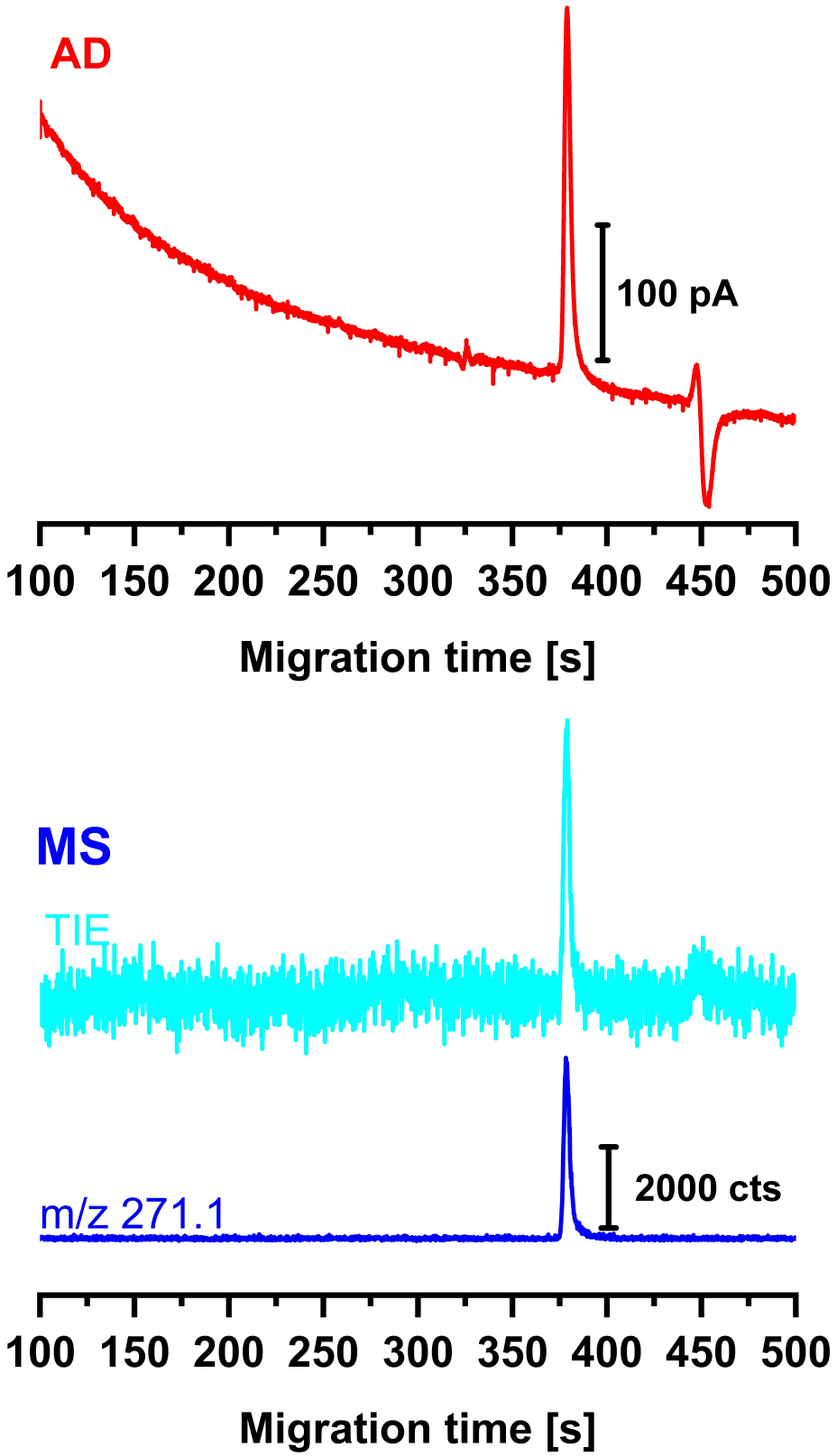

FIGURE 5 CE-AD/MS measurement of the diluted pill extract. The electropherogram at the top was recorded with AD, at the bottom the extracted ion electropherogram of NIT $[M+H]^+$ and the total ion electropherogram (TIE)recorded with MS are shown.

separation, whereby AD provided a high degree of sensitivity. Quantitative determinations were based on external calibration taking advantage of the very good stability of non-aqueous AD. Furthermore, no loss in

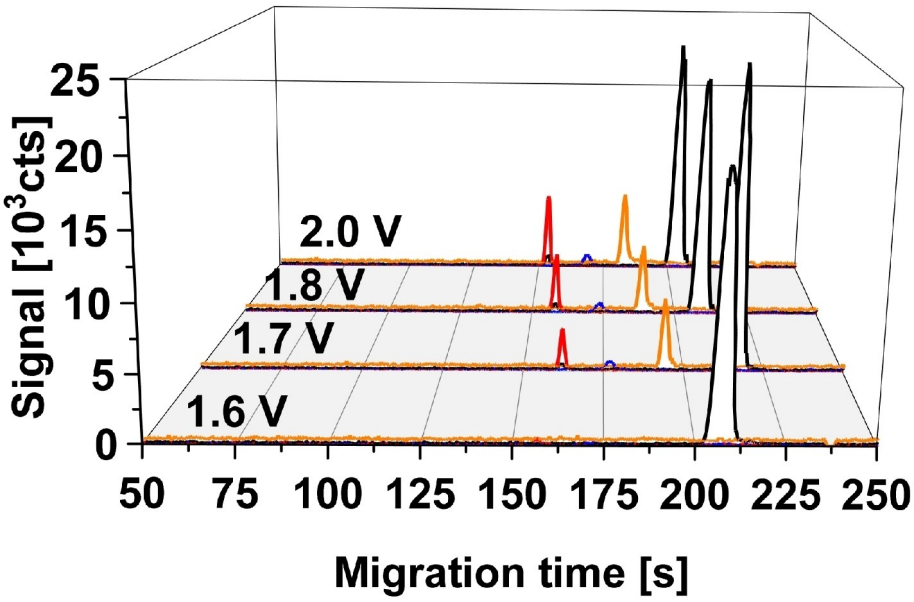

FIGURE 6 EC-CE-MS measurements of 0.1 mM NIT in ACN BGE at different potentials. Extracted ion electropherograms of the product species *m/z* 270.096 (red), *m/z* 258.096 (blue), *m/z* 141.111 (orange), and NIT ($[M+H]^+$, black).

sensitivity was found due to the flow splitting. The advantages of the DDC could be shown using the example of a pesticide pill developed for pets. Combined with a suitable extraction technique, the product could be examined for impurities, and at the same time, the active substance NIT could be sensitively quantified within one measurement. Additionally, we were able to provide an extraction technique for NIT in pill matrices, yielding high recovery rates.

The possible application of the DDC is not limited to pills. In future applications, other NIT-containing samples like water, soil, or plant materials could be examined using CE-AD/MS combined with suitable sample preparation.

Furthermore, as part of this study, a new and versatile CE system was presented, which offers numerous possibilities for optimization in method development. Due to its modular design, the CE system can be upgraded with many modules and various detectors. This could be shown using the example of the electrochemical injection unit. With the combined method, short-lived species could also be formed and investigated. The platform created in this way can be further expanded and improved during the injection of the samples and the detection to increase its versatility and user-friendliness.

ACKNOWLEDGMENTS

The authors thank Mr. Josef Kiermaier (Central Analytical Department, University of Regensburg) for his support in performing the EC-CE-MS measurements.

The authors thank the staff of the electronic and mechanical workshops of the faculty of chemistry and pharmacy (University of Regensburg) for their help in developing and constructing the novel CE device.

We are grateful to the Deutsche Forschungsgemeinschaft (DFG, German research foundation) for financial support (project number MA1491/12-1).

CONFLICT OF INTEREST STATEMENT

The authors declare no conflicts of interest.

DATA AVAILABILITY STATEMENT

The data that support the findings of this study are available from the corresponding author upon reasonable request.

REFERENCES

1. J. E. Casida, *Annu. Rev. Entomol.* **2018**, *63*, 125.
2. L. R. Hovda, S. B. Hooser, *The Veterinary clinics of North America. Small animal practice* **2002**, *32*, 455.
3. P. Jeschke, R. Nauen, M. Schindler, A. Elbert, *J. Agric. Food Chem.* **2011**, *59*, 2897.
4. a) T. Blacquière, G. Smagghe, C. A. M. van Gestel, V. Mommaerts, *Ecotoxicology* **2012**, *21*, 973; b) M.-P. Chauzat, A.-C. Martel, N. Cougoule, P. Porta, J. Lachaize, S. Zeggane, M. Aubert, P. Carpentier, J.-P. Faucon, *Environ. Toxicol. Chem.* **2011**, *30*, 103; c) A. Decourtye, J. Devillers, E. Genecque, K. Le Menach, H. Budzinski, S. Cluzeau, M. H. Pham-Delègue, *Arch. Environ. Contam. Toxicol.* **2005**, *48*, 242; d) A. Decourtye, E. Lacassie, M.-H. Pham-Delègue, *Pest Manage. Sci.* **2003**, *59*, 269.
5. a) D. Loser, K. Grillberger, M. G. Hinojosa, J. Blum, Y. Haufe, T. Danker, Y. Johansson, C. Möller, A. Nicke, S. H. Bennekou et al, *Arch. Toxicol.* **2021**, *95*, 3695; b) E. Bivehed, A. Gustafsson, A. Berglund, B. Hellman, *Expo Health* **2020**, *12*, 547; c) D. A. Thompson, H.-J. Lehmler, D. W. Kolpin, M. L. Hladik,

J. D. Vargo, K. E. Schilling, G. H. LeFevre, T. L. Peeples, M. C. Poch, L. E. LaDuca et al, *Environ. Sci. Process. Impacts* **2020**, *22*, 1315.
6. K. Mao, X. Zhang, E. Ali, X. Liao, R. Jin, Z. Ren, H. Wan, J. Li, *Pestic. Biochem. Physiol.* **2019**, *157*, 26.
7. a) J. Ge, Y. Xiao, Y. Chai, H. Yan, R. Wu, X. Xin, D. Wang, X. Yu, *Ecotoxicol. Environ. Saf.* **2018**, *162*, 423; b) I. Ahmed, C. F. A. Vogel, G. Malafaia, *Sci. Total Environ.* **2022**, *804*, 150254.
8. H. Obana, M. Okihashi, K. Akutsu, Y. Kitagawa, S. Hori, *J. Agric. Food Chem.* **2002**, *50*, 4464.
9. A. Yar, T. M. Ansari, A. Raza, Z. Javeed, M. Asif, *Liaoning Gongcheng Jishu Daxue Xuebao Journal of Liaoning Technical University (Natural Science Edition)* **2023**, *19*, 81.
10. N. Muhammad, Y. Zhang, W. Li, Y.-G. Zhao, A. Ali, Q. Subhani, T. Mahmud, J. Liu, H. Cui, Y. Zhu, *J. Sep. Sci.* **2018**, *41*, 4096.
11. a) M. Noestheden, S. Roberts, C. Hao, *Rapid Commun. Mass Spectrom.* **2016**, *30*, 1653; b) V. I. Iancu, T. Galaon, M. Niculesco, C. Blaziu Lehr, *Rev. Chim.* **2017** *68* 8.
12. L. Sánchez-Hernández, D. Hernández-Domínguez, J. Bernal, C. Neusüß, M. T. Martín, J. L. Bernal, *J. Chromatogr. A* **2014**, *1359*, 31.
13. D. Böhm, M. Koall, F.-M. Matysik, *Electrophoresis* **2023**, *44*, 492.
14. D. Böhm, M. Koall, F.-M. Matysik, *Electrophoresis* **2022**, *43*, 1438.
15. F.-M. Matysik, *Electrophoresis* **2002**, *23*, 40.
16. a) F.-M. Matysik, *Microchim Acta* **2008**, *160*, 1; b) J. J. P. Mark, R. Scholz, F.-M. Matysik, *J. Chromatogr. A* **2012**, *1267*, 4.
17. F. M. Matysik, *J. Chromatogr. A* **1999**, *853*, 27.
18. C. V. Oprea, M. Popa, N. Hurduc, *Polym. J.* **1984**, *16*, 191.

SUPPORTING INFORMATION

Additional supporting information can be found online in the Supporting Information section at the end of this article.

How to cite this article: M. Koall., D. Böhm, T. Herl, F.-M. Matysik, *Electroanalysis* **2023**, *35*, e202300238. https://doi.org/10.1002/elan.202300238

Graphical Abstract

The contents of this page will be used as part of the graphical abstract of html only.
It will not be published as part of main.